Modeling, Identification and Control, Vol. 45, No. 2, 2024, pp. 65–81, ISSN 1890–1328

Investigating the performance of Robust Daily Production Optimization against a combined well–reservoir model

N. Janatian [1] S. Krogstad [2] R. Sharma [1]

[1] *Department of Electrical Engineering, Information Technology and Cybernetics, University of South-Eastern Norway, Porsgrunn, Norway. E-mail:* {nima.janatian,roshan.sharma}@usn.no

[2] *Department of Mathematics and Cybernetics, SINTEF Digital, Oslo, Norway. E-mail:* stein.krogstad@sintef.no

Abstract

This paper presents a scenario-based optimization framework applied to Daily Production Optimization (DPO) for an Electric Submersible Pump lifted oil field under parametric uncertainty. The study also develops a simplified combined well–reservoir model, which is used solely to assess the performance of the methods in a more realistic setting. The combined model consists of the steady-state model of wells combined with the reservoir model through bottom hole pressure and well flow. Moreover, it successfully represents the change in uncertain parameters based on reservoir dynamics rather than random variations. The superiority of scenario-based DPO and the importance of considering uncertainty are demonstrated through extensive comparisons between deterministic and robust methods. The comparisons show that the deterministic DPO fails to satisfy output constraints, leading to violations, particularly in wellhead pressure. Conversely, the scenario-based DPO exhibits significant potential for real oil field application, effectively respecting all input and output constraints. Nevertheless, this safety comes at the cost of sacrificing net profit to some extent. The research emphasizes the importance of considering uncertainty in DPO for oil field operations, providing valuable insights for achieving robustness and operational safety.

Keywords: ESP Lifted Oil Well, Scenario-based Robust Optimization, Constrained Optimization under Uncertainty, The MATLAB Reservoir Simulation Toolbox (MRST), Combinded Well–Reservoir Model

1 Introduction

Decisions made at various time scales have a significant impact on the cost and revenue of an oil and gas production unit. Depending on the goals, these decisions can span from immediate choices made in seconds to long-term plans encompassing the entire lifespan of the field. Daily Production Optimization (DPO), also known as Real-Time Optimization (RTO) in the context of process systems, corresponds to the decisions and plans that are taken within a timeframe ranging from a few hours to a couple of days to maximize the daily operating revenue from the production unit. Typical decisions in this area involve selecting the choke opening of the different wells or allocating shared resources such as available electric power and lift gas. These decisions aim to maximize the daily operational profit while simultaneously ensuring the fulfillment of process and operating constraints Krishnamoorthy et al. (2019). Studies have reported the advantageous impact of daily production optimization, resulting in an increase in production within the range of 1-4% Stenhouse et al. (2010); Teixeira et al. (2013). These improvements are even more pronounced for fields in the late plateau and decline phases than ear-

doi:10.4173/mic.2024.2.3

lier phases Foss et al. (2018). On the other hand, it is widely acknowledged that real-life implementations of constrained optimization may be jeopardized by the presence of uncertainty as the mismatch introduced due to uncertainty may potentially lead to constraint violation and make an optimal solution practically infeasible Janatian and Sharma (2023a); Janatian et al. (2022). Thus, this paper aims to extend the current boundaries of daily production optimization under uncertainty one step further by investigating the daily production optimization problem for an Electric Submersible Pump (ESP) lifted oil field under the presence of uncertainty to bring it closer to practical implementation in real-world scenarios.

Mathematical modeling of a single ESP oil well was proposed in Pavlov et al. (2014). Furthermore, a linear model predictive control (MPC) was designed in the Statoil Estimation and Prediction Tool for Identification and Control (SEPTIC) based on the step response model of the process, which was later implemented on a Programmable Logic Controller (PLC) in Binder et al. (2014). It was shown in Krishnamoorthy et al. (2016a) that the linear model of an ESP lifted well varies significantly depending on the choke opening. Therefore, a model adaptation based on the homotopic transition between models was proposed in Delou et al. (2019), where an adaptive linear MPC strategy was implemented as a Quadratic Dynamic Matrix Control (QDMC) algorithm in order to control the pump inlet pressure, minimizing the pump power and respecting the variable's constraints. An adaptive infinite horizon MPC strategy was also implemented in Santana et al. (2021), where the proposed control law used successive linearization of the dynamic model of ESP to update the model internally. The ESP model was used in Binder et al. (2019) to investigate the implementation aspects of measured disturbances in MPC. The main control objective in this work was to sustain a given production rate from the well while maintaining acceptable operating conditions for the pump. Recently, an Echo State Neural Network was trained in Jordanou et al. (2022) to capture the dynamic model of ESP well. The trained neural network was used for two nonlinear model predictive controllers that aimed to track the bottom-hole pressure subject to constraints on control inputs, bottom-hole and well-head pressures, and liquid flows. Nevertheless, the control presented in the aforementioned studies aimed to track a certain set point (mostly bottom-hole pressure). This type of objective corresponds to the lower layer (Control and Automation layer as described in Foss et al. (2015)) in the multilevel control hierarchy, where the set points are determined by the higher level called Production Optimization to be tracked. Therefore, none of these works have answered the principal question of DPO, which is: *What is the optimal production allocation from each well to maximize the overall economic objective?*

A similar first principle model was developed in Sharma and Glemmestad (2014b) for multiple ESP wells that share a common production manifold. The steady-state version of this model was used in Sharma and Glemmestad (2013) to develop a nonlinear optimization based on Sequential Quadratic Programming (SQP) for two optimal control strategies. The same model was used later in Sharma and Glemmestad (2014a) to calculate and identify the number of oil wells that should be used for special cases with low production demand by formulating a Mixed Integer Nonlinear Programming problem (MINLP). The dynamic version of the model was also exploited in Sharma and Glemmestad (2014c), where the nonlinear model predictive control framework was implemented as an economic optimizer for maximizing profit. Despite assuming constant controls throughout the prediction horizon, the length of the prediction horizon was restricted to one second due to the fast dynamics of ESP and the significant computational expenses associated with a longer prediction horizon. Furthermore, the uncertainty was neglected, while it is well known that the uncertainty in the parameters can make the optimal solution practically infeasible due to the mismatch between the prediction model and the real process Janatian and Sharma (2023b).

In spite of the numerous studies on daily production optimization, such as Mohammadzaheri et al. (2016); Mejía et al. (2018); Epelle and Gerogiorgis (2019); Hoffmann and Stanko (2017); Müller et al. (2022) to name a few, the uncertainty has rarely been taken into account in the optimization problem explicitly. Therefore this paper aims to fill this knowledge gap by extending our previous research work presented in Janatian and Sharma (2023c) by incorporating a more sophisticated representation of the actual plant in order to facilitate the implementation of the method in real-life application. To accomplish this objective, the scenario-based optimization framework has been used in this paper for robust optimization under uncertainty. The Principal aspect of the method involves incorporating a scenario tree to represent finite realizations of uncertainty. The method was integrated into a nonlinear model predictive control scheme in Lucia et al. (2013) for dynamic optimization of semi-batch polymerization reactor under uncertainty. It was also used in the domain of oil production to optimally allocate a limited amount of available lift gas between multiple wells in a gas-lifted oil field Janatian and Sharma (2022); Krishnamoorthy et al. (2016b). However, using the dynamic model of ESP for DPO becomes problematic since the fast dy-

namics of the pumps require a short sampling time, and the number of decision variables over a relatively long horizon, such as in DPO, becomes intractable. Accordingly, the piecewise steady operation of the plant is assumed throughout the prediction horizon. More specifically, the prediction horizon of DPO is divided into segments, and the plant is considered to operate at a possibly new steady state over each segment. Therefore, the steady-state model of the plant is used as the prediction model to determine the future of the system over each segment. The authenticity of this assumption is discussed thoroughly in Foss et al. (2018); Janatian and Sharma (2023c), which state that successive static optimization suffices in most relevant DPO cases and the ESP system is sufficiently fast that the transition between steady states is negligible and can be disregarded. As a result, the daily production optimization is formulated as successive scenario-based optimization problems in a receding horizon fashion to address the constraint fulfillment under the presence of uncertainty. In other words, only the first optimal decision is implemented in the plant, and the whole optimization process will be repeated at each time step.

Although both the current and previous work in Janatian and Sharma (2023c) make use of a simple linear well flow model with productivity index and water cut in the optimization problem, the distinction between the two works lies in the inclusion of a more advanced plant model in this work to accurately portray the actual process. To this end, a reservoir model is coupled in a simple and efficient way to represent the real process. Particularly, instead of testing the optimization algorithm against the same linear model with different parameters, a coupled well-reservoir model is tailored to evaluate the performance of the optimization algorithm. Thus, this work contributes to two major aspects:

- First, incorporating the explicit notion of uncertainty in DPO as a short-term production optimization.
- Second, investigating the performance of the method against a more sophisticated representation of the real process.

The rest of the paper is organized as follows. Section 2 describes the process, including the mathematical modeling of the ESP oil wells and the coupled well–reservoir model. The problem formulations for both standard deterministic DPO and robust scenario-based DPO are presented in Section 3. The considered case study and the simulation setup are presented in Section 4. The simulation results are presented and discussed in Section 5 before concluding in Section 6.

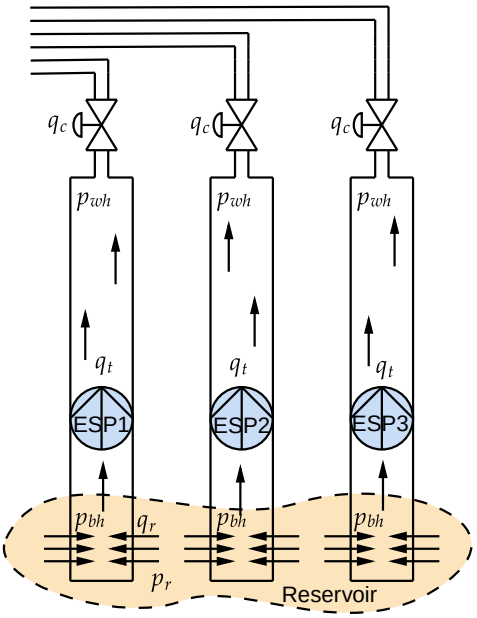

Figure 1: Schematic diagram of three ESP lifted oil wells.

2 Process Description

2.1 ESP Lifting Method

ESP lifting method is an ideal artificial lifting method for producing substantial quantities of dense and viscous hydrocarbons Takacs (2017). In this method, an electrical submersible multistage centrifugal pump is installed at the bottom of the wellbore Sharma and Glemmestad (2014b) to produce the required pressure gradient for bringing the fluid to the surface. A schematic diagram of ESP lifted production unit with three oil wells is presented in Figure 1. Each well, as demonstrated in Figure 1, is equipped with a separate ESP unit at the bottom hole and a production chock valve at the wellhead. During normal operation, the volumetric production rate of individual wells can be regulated by adjusting the pump speed, as it is more beneficial to maintain the production choke valves in a fully open position. Eventually, the oil produced from each well is routed through the top-side network toward the separator for further processing.

Simple mechanistic models of ESP-lifted oil wells are developed in Pavlov et al. (2014); Sharma and Glemmestad (2014b) for optimization and control purposes. Both models are derived by applying the mass and momentum balance principles to the pipelines. This paper considered a similar mathematical model adopted from Sharma and Glemmestad (2014b) with minor adjustments made to certain assumptions:

- Modeling the electrical motors subsystem is neglected due to the fast response of electrical systems.
- Water cuts of the wells are considered to be different to draw a meaningful optimization problem.
- Modeling the common production manifold and transportation lines are neglected, as it is elaborated upon below.

It is worth mentioning that the well model, in a nutshell, is nothing but a flow model through a pipe. And it is typically defined by two boundary pressures, namely the reservoir pressure on one end and the separator or manifold pressure on the other end. However, for the considered model in this paper, the top-side boundary pressure is discarded, and two boundary conditions are considered at the bottom hole, namely the boundary pressure (bottom hole pressure) and boundary flow (reservoir inflow). As a result, the production choke valve is excluded, and the top-side pressure (wellhead pressure) is treated as a free variable. The justification for this assumption is threefold:

- Firstly, the well model is going to be coupled with the reservoir model through the flow and pressure at the bottom hole; therefore, specifying a boundary pressure at the top side of the well model results in an overdetermined subsystem.
- Secondly, the main objective of this paper is to find the optimal production from each well that maximizes the total economic profit, and routing the produced fluid through the top-side network toward the separator falls out of the scope of this paper. Accordingly, putting constraints on the wellhead pressure is sufficient to address the top-side operational constraint in this work.
- Finally, although a more sophisticated coupling between the well model and reservoir model could be possible, it requires solving both the reservoir and well model simultaneously. This is computationally expensive and makes the optimization problem intractable.

2.2 Governing Equations

This section only briefly presents the governing equations of the process since modeling is not the main focus and contribution of this work. However, the readers are referred to Sharma and Glemmestad (2014b) for a more detailed explanation of the modeling.

The process is described by three states for each well, namely, the pressure at the bottom hole p^i_{bh}, the pressure at the wellhead p^i_{wh}, and the average volumetric flow rate of the well q^i_t, where the superscript i refers to the i^{th} oil well. The corresponding differential equations are given by:

$$\dot{p}^i_{bh} = \frac{\beta}{V^i}\left[q^i_r - q^i_t\right] \tag{1a}$$

$$\dot{p}^i_{wh} = \frac{\beta}{V^i}\left[q^i_t - q^i_c\right] \tag{1b}$$

$$\dot{q}^i_t = \frac{A^i}{\rho^i_l L^i}\left[p^i_{bh} - p^i_{wh} + \rho^i_l g H^i_{esp} - \rho^i_l g L^i - \Delta p^i_f\right] \tag{1c}$$

The steady-state equations of the model can simply be determined by setting the right-hand side of differential equations (1) to zero.

$$q^i_r - q^i_t = 0 \tag{2a}$$

$$q^i_t - q^i_c = 0 \tag{2b}$$

$$p^i_{bh} - p^i_{wh} + \rho^i_l g H^i_{esp}(q^i_t, f^i) - \rho^i_l g L^i - \Delta p^i_f = 0 \tag{2c}$$

And the set of algebraic equations is given by:

$$q^i_r = PI^i\left(p_r - p^i_{bh}\right) \tag{3}$$

$$\Delta p^i_f = \frac{f_D L \rho \upsilon^2}{2D_h} \tag{4}$$

$$H^i_{esp} = \bar{c}_0(\frac{f}{f_0})^2 + \bar{c}_1(\frac{f}{f_0})q^i_t + \bar{c}_2 {q^i_t}^2 + \bar{c}_3(\frac{f_0}{f}){q^i_t}^3 \tag{5}$$

$$BHP^i_{esp} = \hat{c}_0(\frac{f}{f_0})^3 + \hat{c}_1(\frac{f}{f_0})^2 q^i_t + \hat{c}_2(\frac{f}{f_0}){q^i_t}^2 + \hat{c}_3 {q^i_t}^3 + \hat{c}_4(\frac{f_0}{f}){q^i_t}^4 \tag{6}$$

$$\rho^i_l = WC^i\rho_w + (1 - WC^i)\rho_o \tag{7}$$

$$q^i_o = (1 - WC^i)q^i_t \tag{8}$$

$$q^i_w = WC^i q^i_t \tag{9}$$

All the algebraic variables of the model are introduced in Table 1. The Darcy friction factor f_D in equation (4) can be evaluated using Serghides' explicit approximation to Colebrook-White equation Serghides (1984). The polynomial coefficients of ESP in equations (5) and (6) are also presented in Table 2 and all the numerical values of the parameters are presented in Table 3.

Note that the model is described by a set of algebraic equations presented in eqs. (2) to (9), which can be encapsulated in a compact form as:

$$\mathbf{F}(x, u, d) = \mathbf{0} \tag{10}$$

where $x \in \mathbb{R}^{10n_w}$ and $u \in \mathbb{R}^{2n_w}$ are the algebraic variables and system inputs, and $d \in \mathbb{R}^{2n_w}$ is the vector of the uncertain parameters of the process. n_w represents the number of wells, and bold typeface in (11) means the vector that encompasses that variable for all the wells.

Table 1: List of the algebraic variables and parameters.

Variable	Description
q_r	Volumetric flow rate from reservoir into well
q_t	Volumetric flow rate through well
q_c	Volumetric flow rate through production choke valve
p_{bh}	Bottom hole pressure
p_{wh}	Wellhead pressure
f	Frequency of ESP
H_{esp}	Head developed by ESP
BHP_{esp}	ESP brake horsepower
ρ_l	Density of the fluid in the well
Δp_f	Frictional pressure drop in the pipe
q_o	Volumetric flow rate of oil
q_w	Volumetric flow rate of water
PI	Productivity index
WC	Water cut

Table 2: Polynomial coefficients of ESP.

	$\bar{c}_0 \backslash \hat{c}_0$	$\bar{c}_1 \backslash \hat{c}_1$	$\bar{c}_2 \backslash \hat{c}_2$	$\bar{c}_3 \backslash \hat{c}_3$	$\bar{c}_4 \backslash \hat{c}_4$
H_{esp}	467.248	10.937	-0.212	7.649e-04	
BHP_{esp}	224.988	0.740	-6.884e-04	2.178e-06	-5.469e-09

$$x = \begin{bmatrix} \mathbf{p_{bh}} & \mathbf{p_{wh}} & \mathbf{q_r} & \mathbf{q_c} & \mathbf{q_o} & \mathbf{q_w} \\ \mathbf{H_{esp}} & \mathbf{BHP_{esp}} & \rho_\mathbf{l} & \mathbf{\Delta p_f} \end{bmatrix}^T \tag{11a}$$

$$u = \begin{bmatrix} \mathbf{f} & \mathbf{q_t} \end{bmatrix}^T \tag{11b}$$

$$d = \begin{bmatrix} \mathbf{PI} & \mathbf{WC} \end{bmatrix}^T \tag{11c}$$

2.3 Well–Reservoir Coupling

The interactions between the two main components of the coupled model, namely the reservoir and well models, are demonstrated in the block diagram presented in Figure 2, in which the optimal values of the decision variables are denoted by the $*$ superscript. As shown in this figure, the optimal values of the ESP frequency f^* and production rate q_t^* are calculated by the optimizer and injected into the plant as inputs. More specifically, the optimal production rate q_t^* is fed into the reservoir model as the "well control," while the true response from the reservoir (i.e., true production rate q_t and bottom hole pressure p_{bh}) is utilized alongside the optimal pump frequency f^* in the well model to compute other outputs, such as wellhead pressure p_{wh} and head of the pump H_{esp}, etc.

Employing this straightforward coupled model instead of a well model with synthetic varying parameters makes it possible to benefit from a more accurate representation of the plant by capturing the variation of uncertainty interactively in accordance with the dynamic of the reservoir and its history.

2.4 Uncertainty Description

Given the fact that the water cut and productivity index are computed at every sampling time, and their values at each sampling time are potentially different from their previous values at the previous sampling time, the uncertainty is inherently incorporated into the plant. However, a deviation of $\pm 10\%$ and $\pm 20\%$ from their actual values are added to them, respectively, as demonstrated in Figure 2, to represent the fact that the actual values of the uncertainties are unknown to the controller.

3 Problem Formulation

3.1 Standard Deterministic DPO

This section presents the standard deterministic optimization using the steady-state model over a finite prediction horizon. The plant is assumed to operate in a piecewise steady manner throughout the prediction horizon. This implies that the prediction horizon of DPO is divided into segments, and the plant is considered to operate at a possibly new steady state over

Table 3: List of the parameters and their corresponding values.

Parameter	Value	Unit	Comments
L	2100	[m]	Length of well above ESP
D	0.1569	[m]	Diameter of all pipelines
A	0.0193	[m^2]	Cross section area of all pipelines
ρ_o	900	[kg/m^3]	Density of water
ρ_w	1000	[kg/m^3]	Density of oil
p_r	400	[bar]	Pressure of the reservoir
μ_o	100e-6	[m^2/s]	Kinematic viscosity of oil
μ_w	1e-6	[m^2/s]	Kinematic viscosity of pure water
f_0	60	[Hz]	ESP characteristics ref. freq.
$Q_{f_0,\min}$	161.591	[m^3/d]	ESP minimum flow at ref. freq.
$Q_{f_0,\max}$	395.252	[m^3/d]	ESP maximum flow at ref. freq.

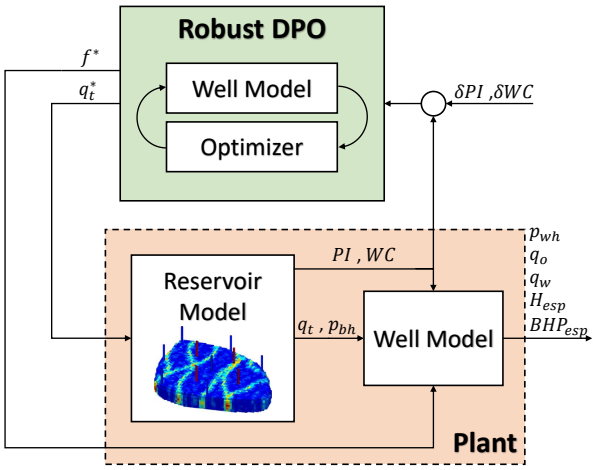

Figure 2: Block diagram of the coupled model and robust optimizer.

each segment.

The primary objective is to adjust the decision variables, namely pump frequencies and inflow to the wells, in order to produce an optimal amount of fluid from each well which maximizes the total profit from the production and takes into account all the operational constraints. Therefore, the economic objective function includes the total income from selling the produced oil with a negative sign to pose it as a minimization problem. Additionally, the costs associated with electric power consumption of the ESPs and water treatment are incorporated into the objective function. Hence, over the prediction horizon $\mathcal{K} = \{1, ..., N_p\}$ with the length N_p the objective function is given by:

$$J_{eco} = \sum_{k=1}^{N_p} \left(-c_o \sum_{i=1}^{n_w} q_o^{i,k} + c_e \sum_{i=1}^{n_w} BHP_{esp}^{i,k} + c_w \sum_{i=1}^{n_w} q_w^{i,k} \right) \tag{12}$$

where c_o, c_e, and c_w denote the price of oil and costs due to the use of electricity and water treatment, respectively.

The most important operational constraints in the problem arise from separator handling capacity and the ESP operating envelope, and the pressures. In particular, the magnitude of produced fluid (comprising both oil and water) should not exceed the separator capacity, and the ESP pumps need to be maintained within a safe operating window to avoid mechanical failure. Additionally, it is required to keep the bottom hole pressure and wellhead pressure within range to ensure the safe operation of the system. Thus, the optimal control problem formulation over the prediction horizon is given by:

$$\min_{\mathrm{x,u}} \quad J_{eco}(\mathrm{x}, \mathrm{u}, \mathrm{d}) \tag{13a}$$

$$\text{s.t.} \quad \mathbf{F}\left(x_k, u_k, d_k\right) = \mathbf{0}, \qquad \forall k \in \mathcal{K} \tag{13b}$$

$$\sum_{i=1}^{n_w} q_t^{i,k} \leq Q_{\text{sep}}, \qquad \forall k \in \mathcal{K} \tag{13c}$$

$$Q_{\min}^{i,k} \leq q_t^{i,k} \leq Q_{\max}^{i,k}, \qquad \forall k \in \mathcal{K} \tag{13d}$$

$$p_{bh}^{\min} \leq p_{bh}^{i,k} \leq p_{bh}^{\max}, \qquad \forall k \in \mathcal{K} \tag{13e}$$

$$p_{wh}^{\min} \leq p_{wh}^{i,k} \leq p_{wh}^{\max}, \qquad \forall k \in \mathcal{K} \tag{13f}$$

$$f_{\min} \leq f^{i,k} \leq f_{\max}, \qquad \forall k \in \mathcal{K} \tag{13g}$$

The equality constraint in (13b) denotes the steady state of the system at each segment of the prediction horizon. The constraint on the total produced fluid is enforced in (13c), where Q_{sep} stands for the maximum handling capacity of the separator. The safe operation of the ESP pumps within the pump envelope is denoted in (13d) by maintaining the pump flow between the minimum and maximum allowed flow which is provided by the ESP manufacturer. The lower and upper bounds on bottom hole pressure and wellhead

pressure are also implemented in (13e) and (13f), respectively. Finally, (13g) ensures the pump frequency is maintained within the range. The optimization problem should be solved in a receding horizon fashion, meaning only the first control action is implemented, and the optimization problem will be solved again at the next sampling time. It should also be noted that the parameters used in the control design are deviated (uncertain) parameters, as the exact values of the parameter are not known.

3.2 Robust Scenario-based DPO

According to the scenario-based optimization approach, the uncertainty region is discretized into a finite number of distinct possible realizations. These realizations are used to evaluate the system's future by employing a scenario tree. This implies that the future evolution of the plant is split into multiple branches, each representing a different trajectory based on the specific realization of the uncertainty that occurs in reality. Nonetheless, the drawback of the method is that the calculations may become intractable as the number of scenarios grows exponentially with the number of considered uncertainty and the length of the prediction horizon. Accordingly, the concept of robust horizon emerged to address this limitation. The robust horizon means the continuation of branching is limited to only a limited number of samples which is typically one or two sampling times ahead in time. The justification for a robust horizon lies in the fact that the corresponding control variables and state trajectories will be recalculated and refined in future sampling times; hence, the far future uncertainty does not need to be represented precisely.

In this paper, the scenario-based optimization method is employed, considering a total of $N_s = 2^6 + 1 = 65$ possible realizations or branches for uncertainties. These realizations encompass all combinations of the maximum and minimum values of the six uncertain parameters and the nominal case. The scenario tree, depicted in Figure 3, illustrates the branching structure with a robust horizon of $N_r = 1$. Each path from the root node to a leaf node represents a scenario; hence the term "scenario-based optimization" is used to describe this method.

It is worthwhile to mention that this formulation imposes an extra constraint which is known as a non-anticipativity constraint. This constraint represents the fact that in real-time decision-making, the decision-maker is not able to anticipate the future realization of the uncertainty. Therefore, all the decisions that branch from a parent node are equal.

After defining the scenario tree and its prerequisites, the objective function for each scenario j can be computed as follows:

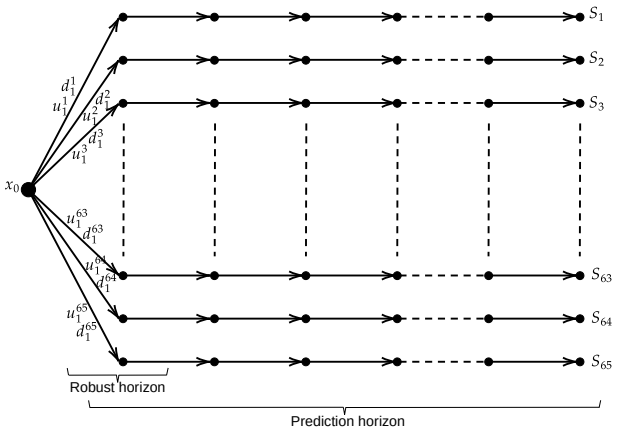

Figure 3: Scenario tree with $N_s = 65$ scenarios and robust horizon $N_r = 1$.

$$J_{eco}^{j} = \sum_{k=1}^{N_p} \left(-c_o \sum_{i=1}^{n_w} q_o^{i,j,k} + c_e \sum_{i=1}^{n_w} BHP_{esp}^{i,j,k} + c_w \sum_{i=1}^{n_w} q_w^{i,j,k} \right) \tag{14}$$

Accordingly, the optimization problem can be formulated over all the discrete scenarios of the scenario set $\mathcal{S} = \{1, ..., N_s\}$, throughout the prediction horizon $\mathcal{K} = \{1, ..., N_p\}$ as follows:

$$\min_{\mathbf{x},\mathbf{u}} \quad \sum_{j=1}^{N_s} \omega_j J_{eco}^{j} \tag{15a}$$

$$\text{s.t.} \quad \mathbf{F}\left(x_k^j, u_k^j, d_k^j\right) = \mathbf{0}, \qquad \forall k \in \mathcal{K}, \forall j \in \mathcal{S} \tag{15b}$$

$$\sum_{i=1}^{n_w} q_t^{i,j,k} \leq Q_{\text{sep}}^{j}, \qquad \forall k \in \mathcal{K}, \forall j \in \mathcal{S} \tag{15c}$$

$$Q_{\min}^{i,k} \leq q_t^{i,j,k} \leq Q_{\max}^{i,k}, \qquad \forall k \in \mathcal{K}, \forall j \in \mathcal{S} \tag{15d}$$

$$p_{bh}^{\min} \leq p_{bh}^{i,j,k} \leq p_{bh}^{\max}, \qquad \forall k \in \mathcal{K}, \forall j \in \mathcal{S} \tag{15e}$$

$$p_{wh}^{\min} \leq p_{wh}^{i,j,k} \leq p_{wh}^{\max}, \qquad \forall k \in \mathcal{K}, \forall j \in \mathcal{S} \tag{15f}$$

$$f_{\min} \leq f^{i,j,k} \leq f_{\max}, \qquad \forall k \in \mathcal{K}, \forall j \in \mathcal{S} \tag{15g}$$

$$u_k^j = u_k^l \quad \text{if} \quad x_k^{p(j)} = x_k^{p(l)}, \quad \forall k \in \mathcal{K}, \forall j \& l \in \mathcal{S} \tag{15h}$$

where J_{eco}^{j} in (15a) is the objective function of the j^{th} scenario and ω_j is the corresponding tuning weight that

reflects the relative likelihood of occurring j^{th} scenario. The steady condition of the system is implemented as a constraint in (15b). It ensures that the states at every time $k \in \mathcal{K}$ from scenario j are at a steady condition which is a function of their corresponding control u_k^j and uncertainty realization d_k^j. The constraints on the separator capacity, pump envelope, and pressures are imposed in (15c), (15d), (15e), and (15f), respectively. And the constraints on the pump frequency are enforced in (15g). Moreover, the non-anticipativity constraint is introduced in (15h), which reflects the fact that at each time step k, controls u_k^j and x_k^l from scenarios j and l with the same parental node $x_k^{p(j)} = x_k^{p(l)}$ have to be equal. In other words, all the controls that are branched from the same parental node are equal. It should be noted that, as shown in Figure 3, branching has been done only for the first sampling time. Therefore, $u_1^1 = u_1^2 = ... = u_1^{64} = u_1^{65}$ is the only set of non-anticipativity constraints in the problem, and according to the receding horizon strategy, this first control action is the one that will be applied to the real system. Hence, the non-anticipativity constraint guarantees that this value is unique.

4 Case Study

4.1 Reservoir Model

The 'Egg Model' is a synthetic reservoir model consisting of an ensemble of 101 relatively small three-dimensional realizations of a channelized oil reservoir produced under water flooding conditions with eight water injectors and four oil producers. The 'standard version' of the model introduced in Jansen et al. (2014) is used as the case study in this paper. The reservoir is demonstrated in Figure 4. The majority of the characteristics of the reservoir, such as rock properties, geometry, etc., remained unchanged. Nevertheless, there are a few minor modifications to meet our requirements. These modifications include:

- The model originally consisted of four production wells and eight injection wells; however, as demonstrated in Figure 4 only three producers are considered in this study.
- The compressibility of oil is set to 1e-3 in order to avoid an unrealistic response.
- The limits on all producer wells are removed as the controller is responsible for satisfying these constraints.
- The injection rate is scaled up to 112.5 [m^3/d] to be consistent with the top side model and requirements.

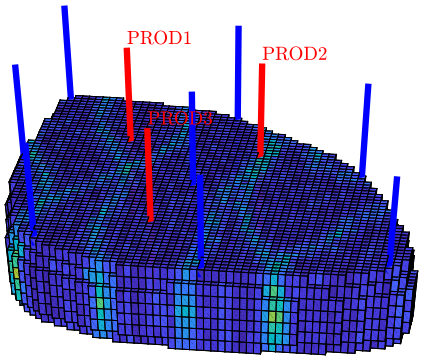

Figure 4: The modified reservoir model with three producers and eight injectors.

- The well control for the producers is changed from bottom hole pressure to total rate, which is provided by the optimizer.

4.2 Simulation Setup

The standard deterministic DPO presented in Section 3.1 and the robust scenario-based DPO proposed in Section 3.2 and a third 'No Control' scenario are simulated to investigate the different aspects of the methods. The so-called 'No Control' scenario, as its name suggests, does not involve any production optimization and assumes the separator capacity is shared equally between three producers. More specifically, each producer produces one-third of the separator capacity. All scenarios are tested against the coupled model in a setup demonstrated in the block diagram of Figure 2.

All the parameters of the wells are presented in Table 2 and Table 3. The price of oil and the costs associated with the electricity and water treatment, which are used in equations (12) and (14), are presented in Table 4. All the sixty-five weights ω_j for sixty-five scenarios in the robust method (15a) are considered to be equally one as all the scenarios are equally likely to occur. The other boundaries of the constraints in the optimization problems defined in (13) and (15) are the same. The separator capacity is considered to be $Q_{\text{sep}} = 900$ [m^3/d]. The bottom hole pressures are considered to be limited between $p_{bh}^{\min} = 200$ [bar] to $p_{bh}^{\max} = 400$ [bar]. The lower and upper limits on the Wellhead pressures are $p_{wh}^{\min} = 150$ [bar] and $p_{wh}^{\max} = 300$ [bar], respectively. The production from each well is limited between $Q_{\min} = 150$ [m^3/d] to $Q_{\max} = 500$ [m^3/d]. The pump frequencies are maintained between $f_{\min} = 45$ [Hz] and $f_{\max} = 80$ [Hz], and

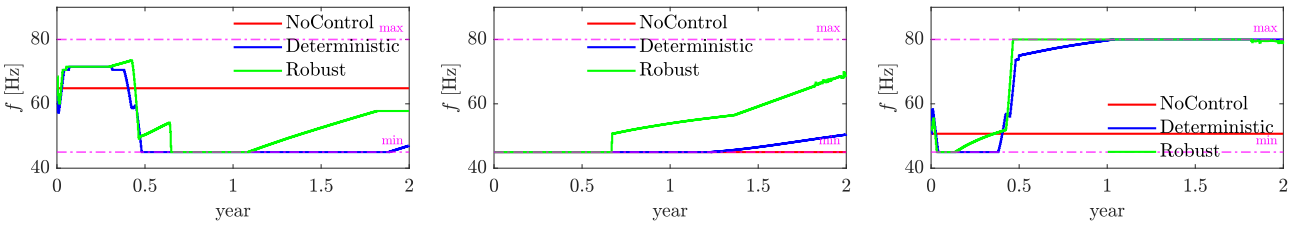

(a) Well 1 (b) Well 2 (c) Well 3

Figure 5: Frequency of ESPs for the production wells.

the pump envelope at each frequency is computed by the affinity law.

A prediction horizon of three days with a sampling time of one day is used for both optimization problems. The optimization problems are implemented in CasADi v.3.5.5 in MATLAB R2022b. The IPOPT v.3.14.1 solver has been used to solve the problem on a 1.8 GHz laptop with 16 GB memory. The MATLAB Reservoir Simulation Toolbox (MRST) Lie and Møyner (2021) has been used for reservoir simulation.

Table 4: Price of oil, electricity, and water treatment.

Price	Value	Unit
c_o	20.03	[$/bbl]
c_e	0.146	[$/kWh]
c_w	3.02	[$/bbl]

5 Results and Discussion

Two simulation cases are conducted to examine various aspects of the method. The first simulation case presents a comparison among three scenarios: deterministic DPO, robust DPO, and the ’No Control’ scenario, which serves as the baseline. The frequency of ESPs for each of these three scenarios is plotted in Figure 5. The other decision variable, which is the production rates, is also Figure 6. It can be seen that all upper and lower bounds are successfully respected, as there is no uncertainty associated with the control inputs. For the same reason, the ESPs for both methods operate within the operating envelope as demonstrated in Figure 7.

However, the other constraint on the outputs, such as the bottom hole and wellhead pressures, may be violated due to the presence of uncertainty. Bottom hole pressures of three scenarios are presented in Figure 8, and the wellhead pressures are presented in Figure 9. The simulation results clearly show that the robust DPO effectively handles the uncertainty, whereas the deterministic DPO leads to constraint violations for a great amount of time.

The subplot (a) in Figure (10) depicts the cumulative profit for each of the three scenarios. In comparison to the baseline scenario, the deterministic DPO shows a total increase of 9.5% in net profit, whereas the robust DPO increases the net profit only by 1.9%. On the other hand, the instantaneous profit from subplot (10b) indicates that both the robust and deterministic DPOs exhibit similar behavior during the initial phases of production. However, as production continues, their divergence becomes more noticeable. Notably, it can be seen from Figure 9 that this differentiation between the two controllers aligns with the constraint violation. In other words, ensuring robust constraint fulfillment comes at a cost, and the price that needs to be paid is to sacrifice potential profit in order to ensure safe and reliable operations.

A second comparison is performed to demonstrate the capability of robust DPO for handling uncertainty. To this end, both methods are tested against the uncertain plant in 20 scenarios with 20 extreme realizations of uncertainty. These uncertainty realizations, as presented in Table 5, are random combinations of the uncertainty bounds. The results of these forty simulations are presented throughout Figure 11 to Figure 15. As depicted in Figure 11 and Figure 12, the frequency and pump flow for both methods remain within the constrained bounds since no uncertainty is associated with the control inputs. Consequently, the pump envelope constraint is successfully fulfilled by both methods, as illustrated in Figure 13. However, the constraint on pressures may be violated. Figure 14 and Figure 15 depict the bottom hole and wellhead pressure, respectively. It can be observed that the constraint on wellhead pressure is violated by deterministic DPO, whereas the robust DPO effectively fulfills the constraint all the time.

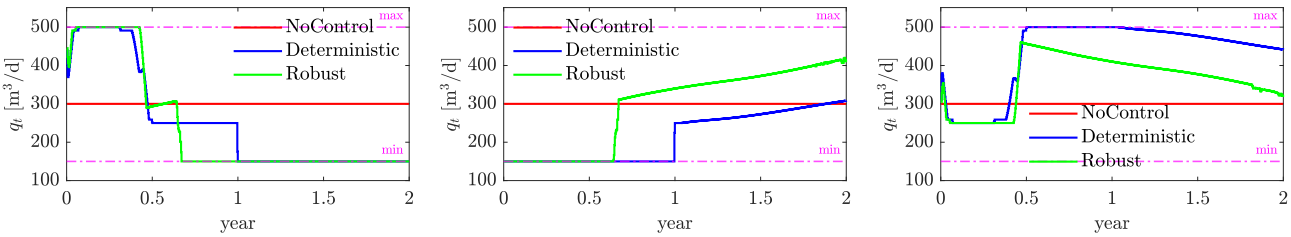

(a) Well 1 (b) Well 2 (c) Well 3

Figure 6: Total fluid flow rates through ESPs in Production wells.

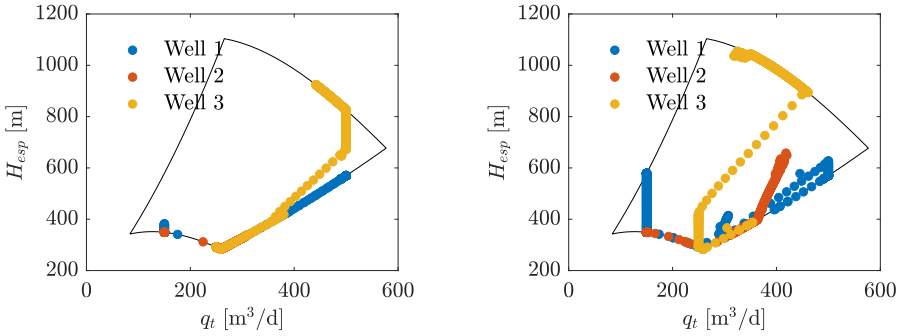

(a) Deterministic DPO (b) Multistage DPO

Figure 7: Operating window of ESPs for different scenarios.

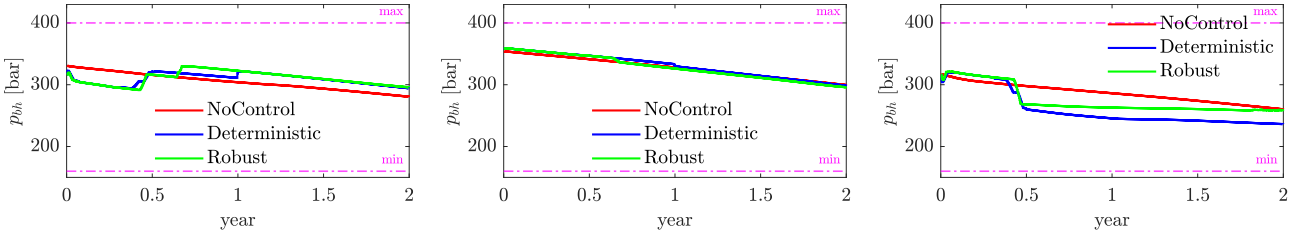

(a) Well 1 (b) Well 2 (c) Well 3

Figure 8: Bottom hole pressure of the production wells.

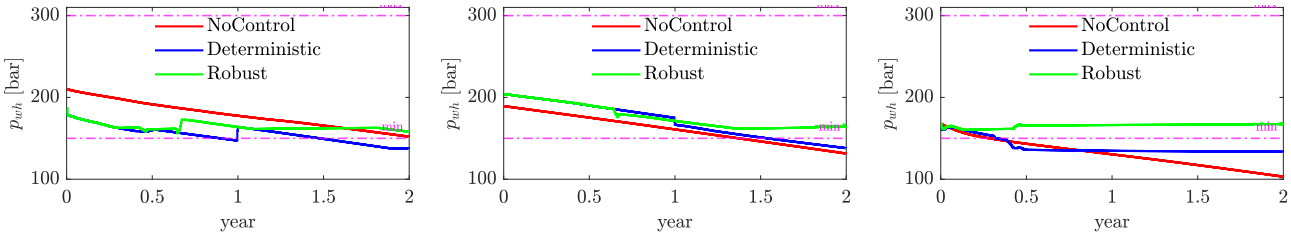

(a) Well 1 (b) Well 2 (c) Well 3

Figure 9: Wellhead pressure of the production wells.

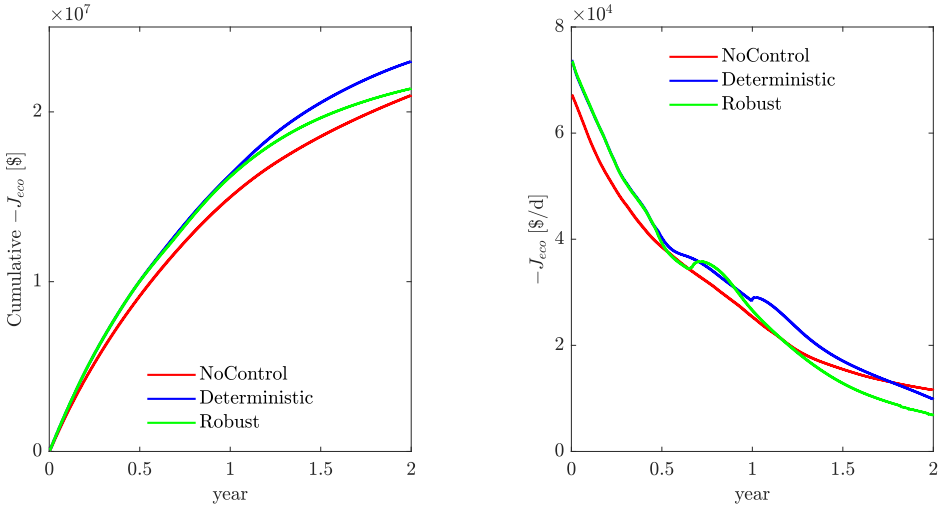

(a) Cumulative profit (b) Instantaneous profit

Figure 10: Net profit ($-J_{eco}$) from production in three scenarios.

Table 5: Twenty random extreme scenarios considered for simulation.

Scenario	δPI^1	δPI^2	δPI^3	δWC^1	δWC^2	δWC^3
1	-10%	-10%	-10%	-20%	20%	-20%
2	10%	10%	-10%	-20%	-20%	-20%
3	10%	-10%	10%	-20%	-20%	-20%
4	10%	-10%	-10%	20%	-20%	-20%
5	-10%	10%	-10%	-20%	20%	-20%
6	-10%	-10%	-10%	20%	-20%	20%
7	10%	10%	10%	-20%	-20%	-20%
8	10%	10%	-10%	20%	-20%	-20%
9	10%	10%	-10%	-20%	20%	-20%
10	10%	-10%	10%	20%	-20%	-20%
11	10%	-10%	10%	-20%	-20%	20%
12	10%	-10%	-10%	20%	-20%	20%
13	-10%	10%	10%	-20%	20%	-20%
14	-10%	10%	-10%	20%	-20%	20%
15	-10%	-10%	10%	20%	-20%	20%
16	10%	10%	10%	20%	-20%	-20%
17	10%	10%	10%	-20%	20%	-20%
18	10%	10%	10%	-20%	-20%	20%
19	10%	10%	-10%	20%	-20%	20%
20	-10%	10%	10%	-20%	20%	20%

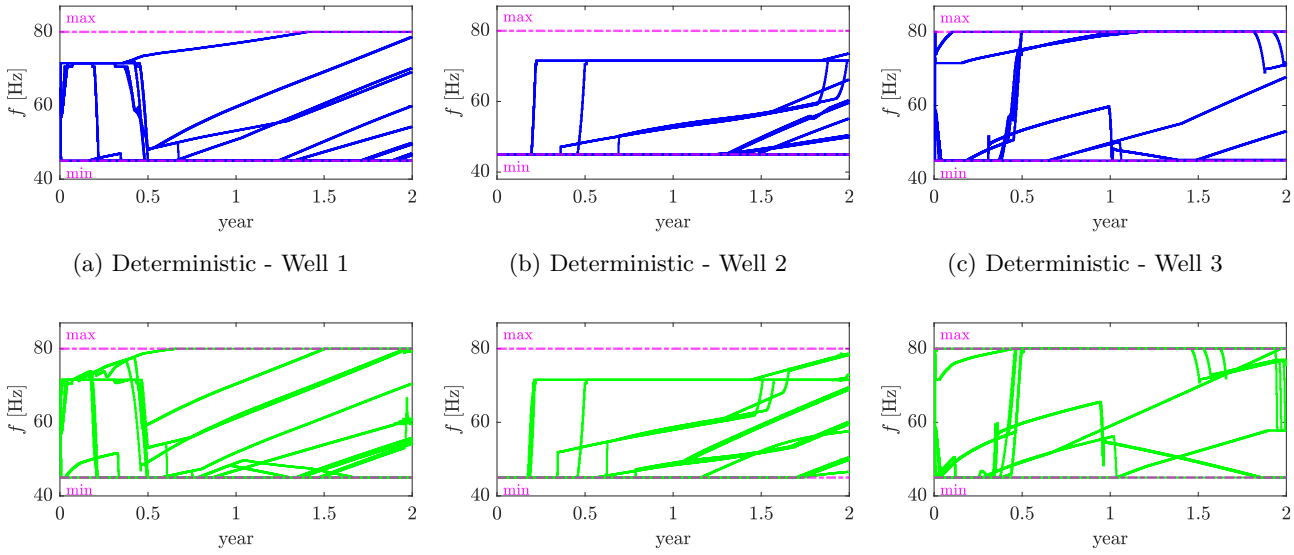

(a) Deterministic - Well 1 (b) Deterministic - Well 2 (c) Deterministic - Well 3

(d) Robust - Well 1 (e) Robust - Well 2 (f) Robust - Well 3

Figure 11: Frequency of ESPs for the production wells.

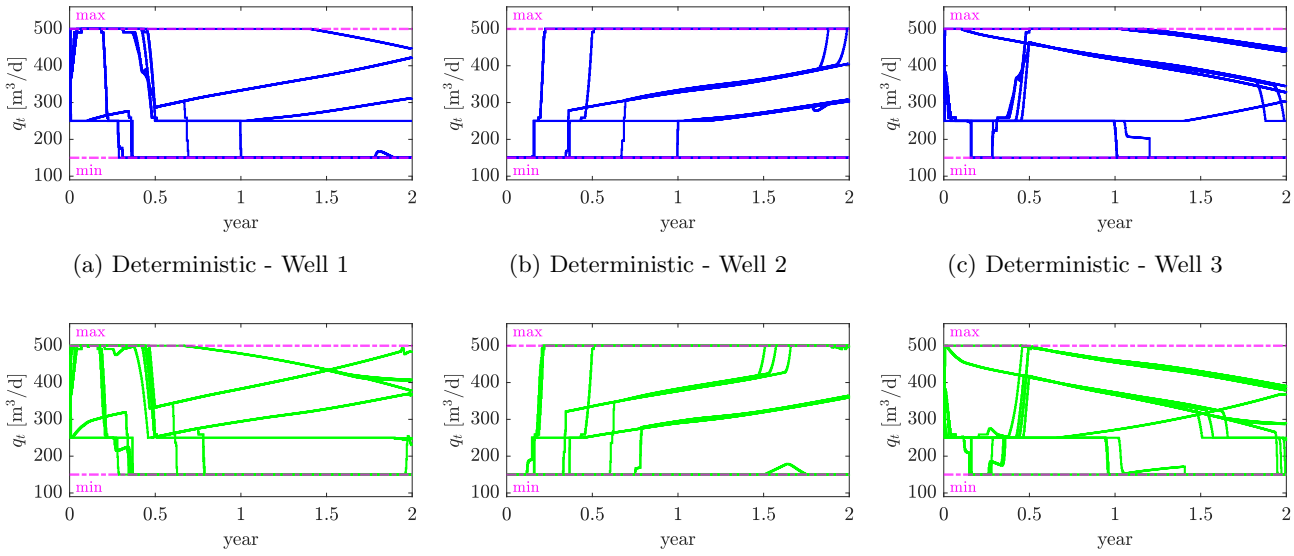

(a) Deterministic - Well 1 (b) Deterministic - Well 2 (c) Deterministic - Well 3

(d) Robust - Well 1 (e) Robust - Well 2 (f) Robust - Well 3

Figure 12: Total fluid flow rates through ESPs in Production wells.

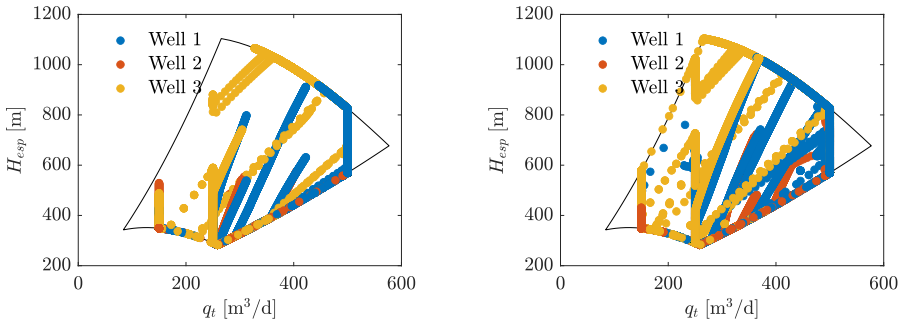

(a) Deterministic DPO (b) Robust DPO

Figure 13: Operating window of ESPs for different scenarios.

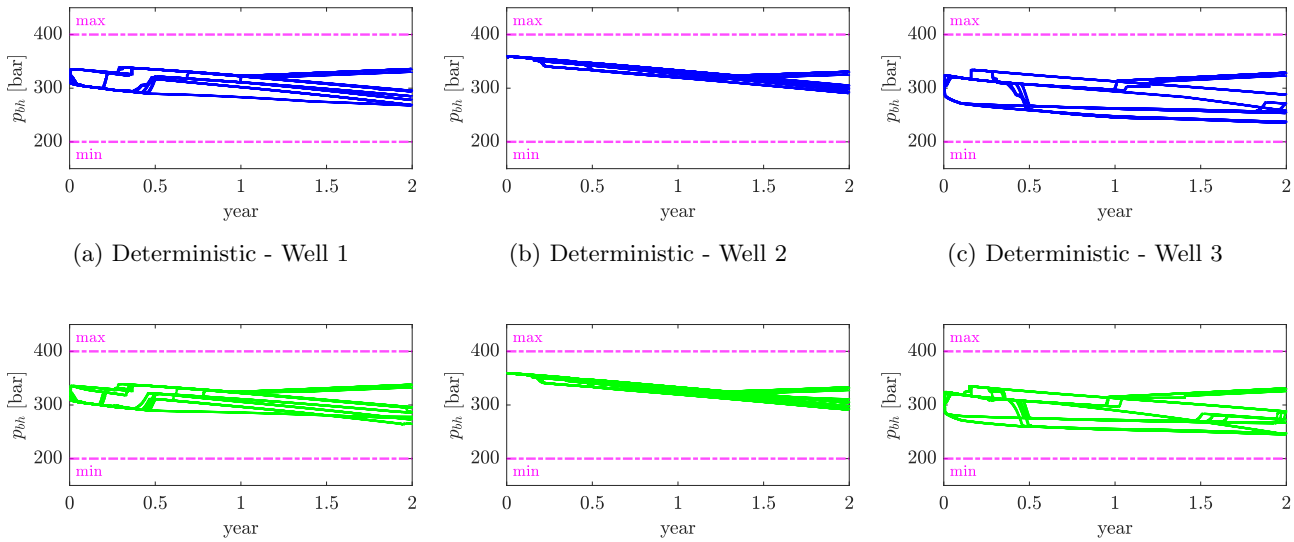

(a) Deterministic - Well 1 (b) Deterministic - Well 2 (c) Deterministic - Well 3

(d) Robust - Well 1 (e) Robust - Well 2 (f) Robust - Well 3

Figure 14: Bottom hole pressure of the production wells.

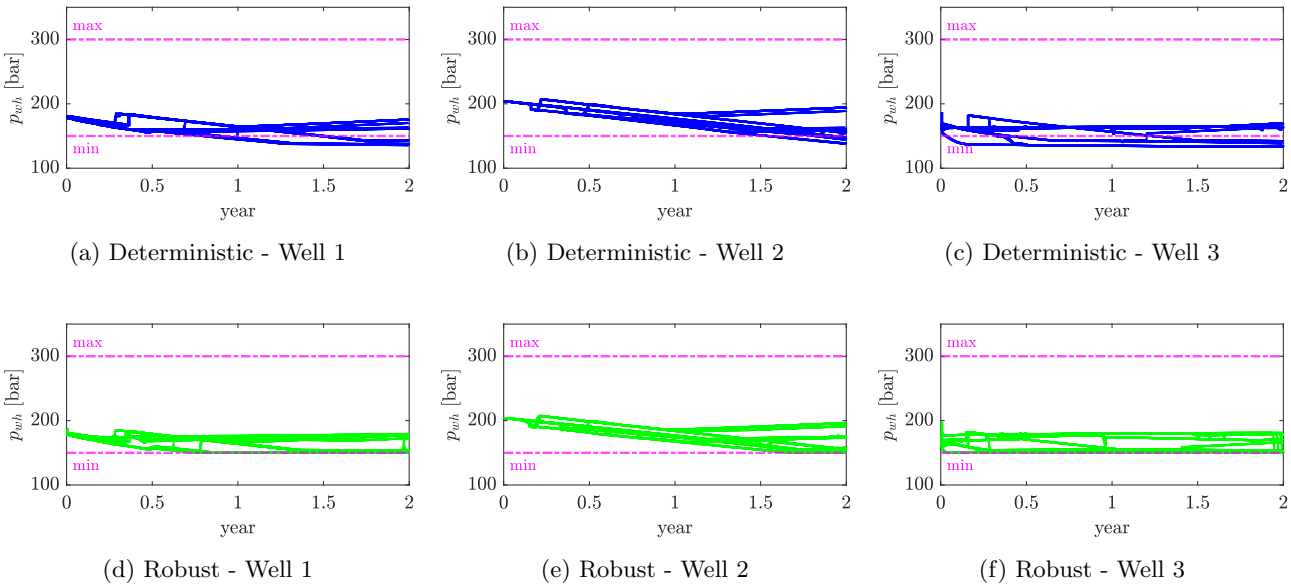

(a) Deterministic - Well 1 (b) Deterministic - Well 2 (c) Deterministic - Well 3

(d) Robust - Well 1 (e) Robust - Well 2 (f) Robust - Well 3

Figure 15: Wellhead pressure of the production wells.

6 Conclusion

This paper utilized the scenario-based optimization framework to address the robust fulfillment of the constraint in Daily Production Optimization for an ESP lifted oil field under parametric uncertainty. Additionally, it presented a simple coupled well–reservoir model to analyze the performance of the method in a more realistic setting.

In order to achieve this objective, the steady-state model of the ESP wells was coupled with the reservoir model in a simple and efficient way. As a result, although the optimization algorithms themselves are based on top-side well models, their performance was evaluated against a more sophisticated model in which the uncertain parameters change interactively in accordance with the dynamic of the reservoir and its history rather than randomly.

The triumph of the proposed method and the importance of considering uncertainty were highlighted through comprehensive comparisons between deterministic and robust DPO applied to the coupled model in the presence of uncertainty. It has been shown that, contrary to the deterministic method, the scenario-based optimization for DPO yields a safe solution, and robust satisfaction of the operational constraints is guaranteed. More specifically, the constraints on pump frequency and flow were fulfilled by both methods, as no uncertainty was associated with the decision variables. However, the simulation results demonstrated that the deterministic DPO is not sufficient for satisfying the constraints on the outputs, and the constraint bounds on some outputs, such as wellhead pressure, were violated. On the other hand, the scenario-based DPO demonstrated a huge potential to be used in a real oil field by effectively respecting all the constraints on both input and output variables. Nevertheless, this safety is achieved at the cost of sacrificing the net profit to some extent.

Despite the contributions of this work, there are potential opportunities for further improvement yet to be explored. The first future direction that should be pursued is to extend the method using Mixed Integer Optimization, which makes it possible to shut down the wells, if it is necessary, as it is reasonably likely that it may be beneficial to shut down some wells during some periods. Another future direction that is worth exploring is to extend the top-side model and consider a more complex network with more oil wells and transportation lines, and gathering manifolds. By pursuing these future directions, the research can further contribute to the field and offer even more valuable insights and solutions for optimizing oil field operations under uncertainty.

Acknowledgments

We gratefully acknowledge the economic support from The Research Council of Norway and Equinor ASA through Research Council project “308817 - Digital wells for optimal production and drainage” (DigiWell).

References

Binder, B. J. T., Johansen, T. A., and Imsland, L. Improved predictions from measured disturbances in linear model predictive control. *Journal of Process Control*, 2019. 75:86–106. doi:10.1016/j.jprocont.2019.01.007.

Binder, B. J. T., Kufoalor, D. K. M., Pavlov, A., and Johansen, T. A. Embedded model predictive control for an electric submersible pump on a programmable logic controller. In *2014 IEEE Conference on Control Applications (CCA)*. IEEE, pages 579–585, 2014. doi:10.1109/CCA.2014.6981402.

Delou, P. d. A., de Azevedo, J. P., Krishnamoorthy, D., de Souza Jr, M. B., and Secchi, A. R. Model predictive control with adaptive strategy applied to an electric submersible pump in a subsea environment. *IFAC-PapersOnLine*, 2019. 52(1):784–789. doi:10.1016/j.ifacol.2019.06.157.

Epelle, E. I. and Gerogiorgis, D. I. Mixed-integer nonlinear programming (minlp) for production optimisation of naturally flowing and artificial lift wells with routing constraints. *Chemical Engineering Research and Design*, 2019. 152:134–148. doi:10.1016/j.cherd.2019.09.042.

Foss, B., Grimstad, B., and Gunnerud, V. Production optimization–facilitated by divide and conquer strategies. *IFAC-PapersOnLine*, 2015. 48(6):1–8. doi:10.1016/j.ifacol.2015.08.001.

Foss, B., Knudsen, B. R., and Grimstad, B. Petroleum production optimization–a static or dynamic problem? *Computers & Chemical Engineering*, 2018. 114:245–253. doi:10.1016/j.compchemeng.2017.10.009.

Hoffmann, A. and Stanko, M. Short-term model-based production optimization of a surface production network with electric submersible pumps using piecewise-linear functions. *Journal of Petroleum Science and Engineering*, 2017. 158:570–584. doi:10.1016/j.petrol.2017.08.063.

Janatian, N., Jayamanne, K., and Sharma, R. Model based control and analysis of gas lifted oil field for optimal operation. *Scandinavian Simulation Society*, 2022. pages 241–246. doi:10.3384/ecp21185241.

Janatian, N. and Sharma, R. Multi-stage scenario-based mpc for short term oil production optimization under the presence of uncertainty. *Journal of Process Control*, 2022. 118:95–105. doi:10.1016/j.jprocont.2022.08.012.

Janatian, N. and Sharma, R. A reactive approach for real-time optimization of oil production under uncertainty. In *2023 American Control Conference (ACC)*. IEEE, pages 2658–2663, 2023a. doi:10.23919/ACC55779.2023.10156274.

Janatian, N. and Sharma, R. A robust model predictive control with constraint modification for gas lift allocation optimization. *Journal of Process Control*, 2023b. 128:102996. doi:10.1016/j.jprocont.2023.102996.

Janatian, N. and Sharma, R. Short-term production optimization for electric submersible pump lifted oil field with parametric uncertainty. *IEEE Access*, 2023c. doi:10.1109/ACCESS.2023.3312169.

Jansen, J. D., Fonseca, R. M., Kahrobaei, S., Siraj, M., Van Essen, G., and Van den Hof, P. The egg model–a geological ensemble for reservoir simulation. *Geoscience Data Journal*, 2014. 1(2):192–195. doi:10.1002/gdj3.21.

Jordanou, J. P., Osnes, I., Hernes, S. B., Camponogara, E., Antonelo, E. A., and Imsland, L. Nonlinear model predictive control of electrical submersible pumps based on echo state networks. *Advanced Engineering Informatics*, 2022. 52:101553. doi:10.1016/j.aei.2022.101553.

Krishnamoorthy, D., Bergheim, E. M., Pavlov, A., Fredriksen, M., and Fjalestad, K. Modelling and robustness analysis of model predictive control for electrical submersible pump lifted heavy oil wells. *IFAC-PapersOnLine*, 2016a. 49(7):544–549. doi:10.1016/j.ifacol.2016.07.399.

Krishnamoorthy, D., Fjalestad, K., and Skogestad, S. Optimal operation of oil and gas production using simple feedback control structures. *Control Engineering Practice*, 2019. 91:104107. doi:10.1016/j.conengprac.2019.104107.

Krishnamoorthy, D., Foss, B., and Skogestad, S. Real-time optimization under uncertainty applied to a gas lifted well network. *Processes*, 2016b. 4(4):52. doi:10.3390/pr4040052.

Lie, K. A. and Møyner, O. *Advanced modelling with the MATLAB reservoir simulation toolbox*. Cambridge University Press, 2021.

Lucia, S., Finkler, T., and Engell, S. Multi-stage nonlinear model predictive control applied to a semi-batch polymerization reactor under uncertainty. *Journal of process control*, 2013. 23(9):1306–1319. doi:10.1016/j.jprocont.2013.08.008.

Mejía, J. A. P., Silva, L. A., and Flórez, J. A. P. Control strategy for oil production wells with electrical submersible pumping based on the nonlinear model-based predictive control technique. In *2018 IEEE ANDESCON*. IEEE, pages 1–6, 2018. doi:10.1109/ANDESCON.2018.8564581.

Mohammadzaheri, M., Tafreshi, R., Khan, Z., Franchek, M., and Grigoriadis, K. An intelligent approach to optimize multiphase subsea oil fields lifted by electrical submersible pumps. *Journal of Computational Science*, 2016. 15:50–59. doi:10.1016/j.jocs.2015.10.009.

Müller, E. R., Camponogara, E., Seman, L. O., Hülse, E. O., Vieira, B. F., Miyatake, L. K., and Teixeira, A. F. Short-term steady-state production optimization of offshore oil platforms: Wells with dual completion (gas-lift and esp) and flow assurance. *Top*, 2022. 30(1):152–180. doi:10.1007/s11750-021-00604-2.

Pavlov, A., Krishnamoorthy, D., Fjalestad, K., Aske, E., and Fredriksen, M. Modelling and model predictive control of oil wells with electric submersible pumps. In *2014 IEEE Conference on Control Applications (CCA)*. IEEE, pages 586–592, 2014. doi:10.1109/CCA.2014.6981403.

Santana, B. A., Fontes, R. M., Schnitman, L., and Martins, M. A. An adaptive infinite horizon model predictive control strategy applied to an esp-lifted oil well system. *IFAC-PapersOnLine*, 2021. 54(3):176–181. doi:10.1016/j.ifacol.2021.08.238.

Serghides, T. Estimate friction factor accurately. *Chemical engineering (New York, NY)*, 1984. 91(5):63–64.

Sharma, R. and Glemmestad, B. Optimal control strategies with nonlinear optimization for an electric submersible pump lifted oil field. *Modeling, Identification and Control*, 2013. 34(2):55–67. doi:10.4173/mic.2013.2.2.

Sharma, R. and Glemmestad, B. Mixed integer nonlinear optimization for esp lifted oil field and improved operation through production valve choking. *International Journal of Modeling and Optimization*, 2014a. 4(6):465. doi:10.7763/IJMO.2014.V4.419.

Sharma, R. and Glemmestad, B. Modeling and simulation of an electric submersible pump lifted oil field. *International Journal of Petroleum Science and Technology*, 2014b. 8(1):39–68.

Sharma, R. and Glemmestad, B. Nonlinear model predictive control for optimal operation of electric submersible pump lifted oil field. In *Proceedings of the IASTED International Conference on Modelling, Identification and Control*. pages 229–236, 2014c. doi:10.2316/P.2014.809-042.

Stenhouse, B., Woodman, M., and Griffiths, P. Model based operational support-adding assurance to operational decision making. In *SPE Intelligent Energy Conference and Exhibition*. OnePetro, pages –, 2010. doi:10.2118/128694-MS.

Takacs, G. *Electrical submersible pumps manual: design, operations, and maintenance*. Gulf professional publishing, 2017.

Teixeira, A. F., de Campos, M., Barreto, F. P., Stender, A. S., Arraes, F. F., and Rosa, V. R. Model based production optimization applied to offshore fields. In *OTC Brasil*. OnePetro, pages –, 2013. doi:10.4043/24301-MS.